Journal of Materials Chemistry C

Accepted Manuscript

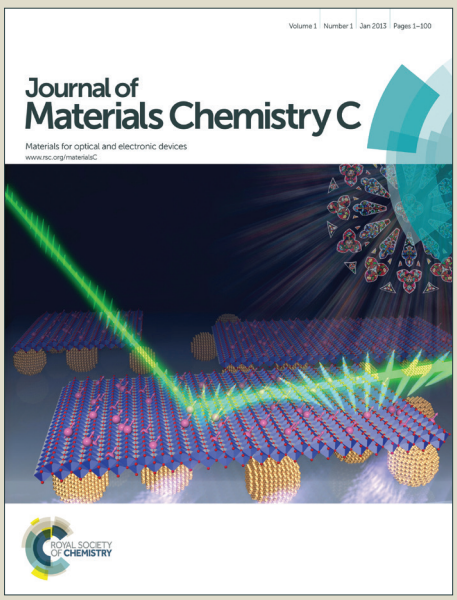

ROYAL SOCIETY OF CHEMISTRY

www.rsc.org/materialsC

Cite this: DOI: 10.1039/c0xx00000x

www.rsc.org/xxxxxx

ARTICLE TYPE

Electron-phonon interaction in bulk layered graphene and its oxide in the presence of alcohols in a device: Equilibrium molecular doping

Sesha Vempati,*[a] Asli Celebioglu[a,b] and Tamer Uyar*[a,b]

Received (in XXX, XXX) Xth XXXXXXXXX 20XX, Accepted Xth XXXXXXXXX 20XX

DOI: 10.1039/b000000x

We report on electron phonon interactions from bulk layered graphene (GRA) and its oxide (GO) under bias when exposed to 1° or 2° alcohol vapors, where we have focused on the change of Raman intensity of G and D bands as a function of the bias across the device. In addition to the softening of phonons we have observed a systematic variation in the intensity for D and G bands which are directly related to *guest* molecules and intrinsic surface nature of GRA and GO. Although the *guest* molecules withdrawn electrons from GRA or GO, the intrinsic nature of *host* material have caused mutually contrasting behaviour in *IV*-characteristics, where the conductance of the former increases while it decreases for the latter. The results from *IV*-spectra and the intensity map of D and G bands are juxtaposed and the changes are analyzed with respect to surface and functional group interactions. In the context of doping, it is interesting to see that under equilibrium molecular charge transfer (top-gate like), the intensity ratios of 2D and G band is not constant in contrast to an earlier study [Phys. Rev. B. vol 80, 165413 (2009)] in which such ratio is invariant in field effect configuration.

Introduction

Graphene based sensors are of recent research interest [1-4] among which detection of single molecule is noteworthy.[3] In any case the sensor works on the basis of change in conductivity of *host* in the presence of a *guest* (test gas).[1,2] The change in conductivity is a result of charge transfer, where two mechanisms are generally possible.[5] They are (i) the relative positions of HOMO/LUMO of *guest* with respect to Fermi level (E_F) of *host* favoring transfer of electrons; or (ii) the mixing of the HOMO/LUMO of *guest* with those of *host* producing hybrid orbitals. In other words, the E_F of graphene is proportional to the square root of the carrier concentration which is shifted when doped because of stiffening or softening of phonons. Note that the phonon dispersion is modified when the carrier concentration and mobility are altered.[6-8] Despite of the fundamental importance of *host-guest* chemistry, the sensitivity of the device is commonly studied for improvements [3,4] which is of course appreciated. The ratio between the intensities of 2D and G peaks from bulk layered graphene (GRA) is almost invariant for various doping densities [9] in field-effect-configuration, however, in the context of molecular charge transfer, we believe that the relative intensity changes of D and G bands of GRA and its oxide (GO) are inevitable to unveil the *host-guest* chemistry. Albeit molecular charge transfer is known when the surface is treated with test molecules [10,11] however, electron-phonon interaction is not well-studied in the presence of *guest* molecules. In this direction *in situ* Raman spectroscopy is employed to detect the electron-phonon interaction [12,13] in the presence of *guest* molecules in a device structure.

Ethanol (EtOH) and isopropanol (IPA) were chosen as model molecules (*guests*) based on the fact that the activity of −OH group depends on the electron directing or withdrawing nature of functional group that it is attached to and the structural differences when a molecule orients on the surface.[3,5,14] Furthermore, the absorption energies against position and orientation are also important factors to consider.[5] See H_2O (acceptor) clusters on graphene for geometric structure and energetics [3,14] in conjunction with gas phase conformers for EtOH (e.g. *trans* and *gauche*) and IPA.[15] *In situ* Raman spectroscopy is performed in the presence of model molecules when GRA and GO are biased in a device structure. We have noticed an anomalous and mutually contrasting behavior of the intensities of G and D bands as well as the conductance of the GRA and GO devices which purely originates from the bias dependence of molecular desorption. Notably, the intercalation of test vapors is not evidenced in the present case from X-ray diffraction studies.[16,17] As expected EtOH and IPA differ from each other in the electron withdrawing nature and clearly show their influence on the intensity of G and D bands from GRA and GO. The results from EtOH and IPA are compared with that of ambient atmosphere (Atm) for detailed understanding. It is also inferred that the intensity ratio, A(2D)/A(G) is not constant for any of the three cases. This study not only addresses the *host-guest* chemistry (or top-gate equilibrium molecular charge transfer) in the potential materials such as GRA and GO, but also suggests a very good platform for computational studies in the context of absorption energies, position and orientation in conjunction with the intensity of G and D bands in a resistive type sensor under

bias. In order to design future generation sensors with the capability of detecting single and selected molecules a better understanding of *host-guest* chemistry is vital,[1-5] especially in the case of bio-sensor applications where target specific sensing is of utmost importance. Starting with smaller molecules such as EtOH and IPA in gas phase may be a wise option to understand such weak interactions using Raman spectroscopy in the background of complex functional groups present on the GO and inevitable edge of GRA.

Experimental

Scanning electron microscopy (SEM) was performed with FEI Quanta 200 FEG. Transmission electron microscopy (TEM) was performed with FEI-Tecnai G2 F30 whiles the samples were dispersed in de-ionized water and a tiny droplet was analyzed from a holey carbon coated TEM grid. X-ray diffraction patterns (XRD) were obtained from PANalytical X'pert Pro MPD (λ = 1.5418 Å). The ionic state of carbon at the surface of the samples was investigated by X-ray photoelectron spectroscopy (XPS, Thermoscientific K-Alpha, Al Kα-hν = 1486.6 eV) with a flood-gun charge neutralizer. Raman spectroscopy was performed with WITec instruments (Alpha 300S, 532 nm laser). Raman-intensities here are the areas under the corresponding peaks which were obtained from Lorentzian shape [9] fitting with Origin 6.1. The center of the peak is chosen manually to initiate the fitting process while the rest of the parameters were set free until convergence. Colloidal dispersion of graphite (Ted Pella, USA) is dried in vacuum and oxidized using an earlier described procedure. [18] The dispersions of GRA or GO are drop-casted on a clean glass slide and electrical contacts were obtained with the same. This device is dried thoroughly in vacuum and then subjected to the electrical characterization (four probe, Figure S1 of ESI) in Atm, EtOH or IPA vapors which were saturated in a closed chamber. *In situ* Raman spectra are recorded from the same chamber for selected bias conditions.

Results and discussion

The SEM images from GRA suggests a typical flake-like structure in contrast with GO which has shown exfoliated nature similar to an earlier observation [19] (Figure S2 of ESI). The sponge like structure is typical to exfoliated graphene. The modified morphology is the primary confirmation of exfoliation, where we can see the influence of the acid treatment as expected.

TEM images are recorded on GRA and GO samples and representative images are shown on Figure 1. From the low resolution images from GRA (Figure 1a) we can see the flake like structure consistent with SEM observation. In Figure 1b GRA has shown very clear overlap of graphene sheets which are nearly straight lines. The distance between the sheets is found to be 3.4 ± 0.06 Å (estimated by measuring 5 planes). SAED pattern (Figure 1c) is recorded on GRA which has shown well defined circles with bright spots, implying predominant crystalline phase. The crystal planes are annotated on the image. It is notable that the layers are perfectly parallel however, their mutual orientation within the plane is random (turbostatic) which is seen as circles in the SAED pattern. The first diffraction ring (002) is slightly diffused revealing that it harbors crystal planes of slightly varying distances. In Figure 1d we have shown HRTEM image from GO, and the stacked planes can be seen which are of course not straight lines like the case with GRA (Figure 1b). This morphology is expected, as the edges are functionalized with various chemical groups [20,21] including the basal plane. The wrinkled morphology is similar to earlier reports [18,22] where the authors have used Brodie process [22] or modified Hummers method [18] to prepare GO. It is also suggested [22] that there may be some un-reacted GRA within the sample, which may be feasible even in the present case.

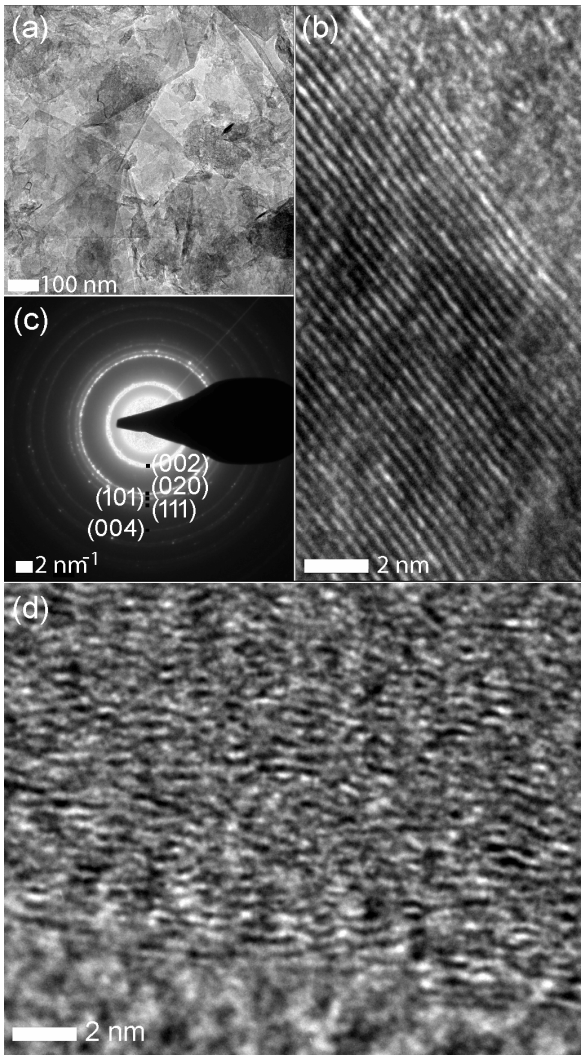

Fig. 1 TEM images from GRA flakes (a) flake like structure, (b) high resolution image showing the various planes which are under π-π bond (c) electron diffraction pattern and (d) corrugated edges from GO.

XRD patterns from GRA and GO samples is shown in Figure 2a and b, while XPS from GO is shown in c. Both the samples have shown sharp diffraction peaks indicating crystalline nature of the samples. The angular location of the peak match with the literature [18,23,24] and the corresponding reflections are annotated on the image. We would like to draw attention to the peak corresponding to (002) reflection (*c*-axis, normal to the hexagonal planes) in both the samples. After oxidation (002) peak has shown a shift to lower 2θ values. Moreover, the second order reflection, (004) can also be seen for both the samples. It is also

interesting to see that the relative intensities of (002) to (004) for GRA case is as high as 33 in contrast to 10 from GrO. This suggests that GO sheets are more random and have been exfoliated successfully. Furthermore, the calculated interplanar spacing (*d*) of GRA and GO are ~3.368 Å and ~9.135 Å, respectively. The lattice spacing for the case of Gr sample is consistent with the measurements from TEM. The *d* value after oxidation depends on the procedure and level of oxidation, while an increase from GRA is a clear consequence of functional group implantation on the basal planes as well as edges of individual graphene sheets.[18] On the other hand, this increase causes a loss in the 3D crystallinity. In contrast to a single (020) reflection from GO, for the case of GRA 40-48˚ region contains multiple peaks (inset of Figure 2(b)).

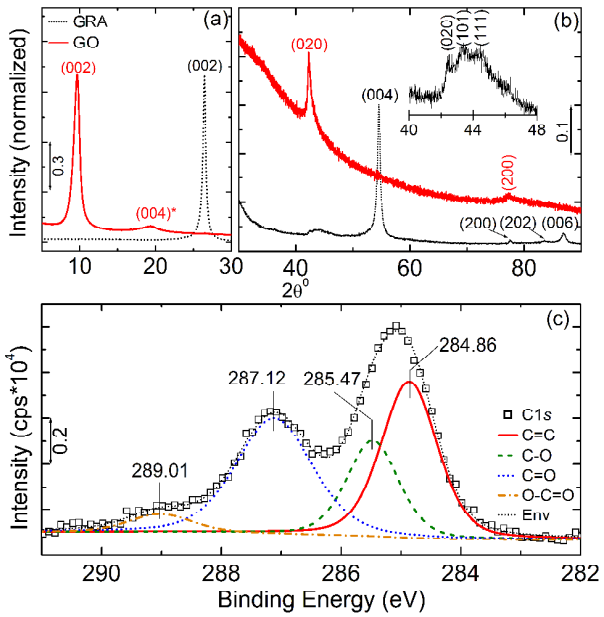

Fig. 2 (Color online) (a) and (b) are XRD pattern from GRA and GO (c) C 1*s* core-level TEM images from GRA flakes (a) flake like structure, (b) high resolution image showing the various planes which are under π-π bond (c) electron diffraction pattern and (d) corrugated edges from GO.

Interestingly, after oxidation these multiple peaks were not present within the detection limits. To re-iterate the aim of this report, we would like to understand the intensity changes in D and G Raman bands in the presence of alcohol vapors while ruling out the formation of intercalated compound is necessary. In the context of intercalation with alcohols,[16,17] *d* has been altered significantly. Hence diffraction analysis is performed on the samples and as an example, the pattern from GRA under EtOH vapor exposure is shown in Figure S3 of ESI. The result suggested null effect on *d*.

The electronic and optical properties of GO and reduced GO depend on the concentration of major functional groups such as epoxides, hydroxyls and carbonyls.[25] For this, we have analyzed C1*s* core-level spectrum to determine the various functional groups as a consequence of the oxidation. Broadly, the spectrum has shown two major and one minor peak (Figure 2c) before deconvolution. The result of the peak deconvolution suggests that the composite peak structure constitute four functional groups *viz* C=C, C-O, C=O and O-C=O. The energetic location of C1*s* in each functional group is annotated on the image, which are found to be in line with the literature.[18] The area ratios are 0.99, 0.56, 1 and 0.13 for C=C, C-O, C=O and O-C=O respectively. As a whole on the surface the sp^2 C=C:oxidized-C ratio of GrO sample is ~1.7:1. During the oxidation the process of oxidation, transfer of charge takes place from GRA to oxygen in all the above functional groups, while the electron density is majorly on the oxygen atom(s) because of its relatively high electronegativity.

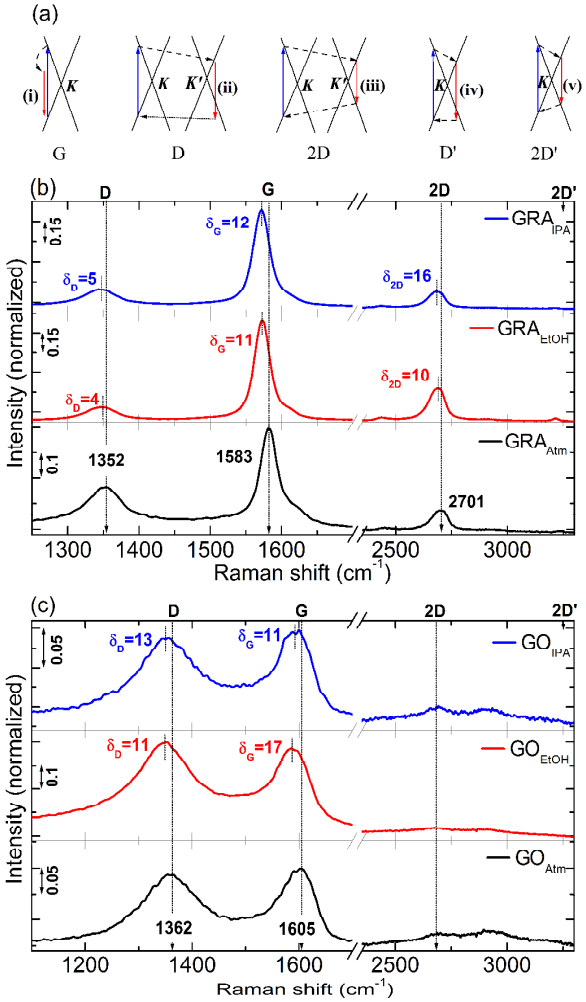

Fig. 3 (Color online) Raman spectra from the devices in three environments for zero bias condition (a) GRA and (b) GO.

The schematic of Raman processes that GRA can host are shown in Figure 3a [9] by following the nomenclature suggested by Ferrari et al.[26] Raman spectra from GRA and GO devices are shown in Figure 3b and c for zero bias condition. The spectral location of each band is annotated on Figure 3a and b which are consistent with the literature.[13,27-29] Contextually, it would be appropriate to discuss the origin of various bands where we refer Figure 3a for all five processes. **(i) G-band:** Originates from sp^2 hybridized C=C bonds [13] and unambiguously assigned to zone centre LO phonon modes of E_{2g} symmetry. The spectral location of this band is independent of excitation energy in the case of GRA.[26,28,30] **(ii) D-band:** Attributed to 'unorganised' carbon and small sized graphite crystals or boundaries of larger crystals,[13] which is essentially the breathing mode of sp^2 atoms in rings.[12,13]

Notably the origin of D-band is attributed variously. *viz* existing selection rules are replaced [26,28,30,31] or a double resonance (DR) phenomenon is introduced.[27] According to Ferrari [28] the DR mechanism [27] is more suitable, which also explains the excitation dependent spectral location of D-peak (due to the Kohn Anomaly at ***K***).[29] **(iii) 2D-band:** An inter valley process and formerly known as G′[26]) however, it is D overtone.[28] **(iv) D'-band:** An intravalley DR process, which connects two points belonging to the same cone around K (or K´). **(v) 2D'-band:** This band corresponds to the second order intra-valley D' peak.

As mentioned in the introduction of this report, the present context deals with the intensity levels of G and D bands. To emphasize the G peak is a one phonon (E_{2g}) process at the Brillouin-zone center. i.e. electron is excited to unfilled state and recombines with hole. Whereas the D peak is an intervalley process due to the breathing modes of six-atom rings activated by a defect. i.e. excitation of an *e/h* pair, electron-phonon scattering with an exchanged momentum, scattering at a defect and finally *e/h* recombination.[9] In this report we will refer each Raman-band as '$Band^{Host}_{Guest}$' and its intensity as 'A($Band^{Host}_{Guest}$)' for simplicity. For example, G band from GRA in the presence of EtOH vapor is referred as G^{GRA}_{EtOH} and its intensity as A(G^{GRA}_{EtOH}). Shifts of each band is annotated with δ where the suffix corresponds to a certain band. 2D band from GRA is found to be almost symmetric (Figure 3b) in contrast to earlier studies [28,31] where clear shoulders corresponding to $2D_1$ and $2D_2$ components are seen. In the case of GO the 2D peak is not seen explicitly apart from a small feature. The crystallite size is calculated to be 106 Å when intensity ratio in Raman signal (I_{1355}/I_{1570} = ~0.44) is taken into account (value estimated from graph).[13] However, this method underestimates the crystallite size due to the dominant effect from small crystallites.[13] Despite, the linear relation [13] suggests that the Raman intensity is proportional to the 'boundary' in the sample. In the case of GO, the comparable intensity of G and D bands is due to increased sp^3 character, see the discussion of XPS results.[32-34] Notably there is no detectable signature of amorphous carbon from GRA and GO (spectral range not shown here). The band G^{GRA}_{Atm} and D^{GRA}_{Atm} have shown a significant red-shift upon exposure to EtOH or IPA vapors. This effect is similar for G^{GO}_{Atm} and D^{GO}_{Atm} cases. Furthermore, G^{GO}_{Atm} is red-shifted from G^{GRA}_{Atm} which can be understood based on the fact that the oxidation removes the electrons from the GRA.[35] Furthermore at an appropriate oxidation level the process may yield a *p*-type semiconductor.[33,36] This oxidation process is permanent where the oxygen functional groups are covalently attached in contrast the presence of EtOH or IPA is temporary via shift of charge carriers. The shift of these bands is because of the change in the carrier concentration and consequently shift of E_F.[6-8] While considering the case with graphene where G band up-shifts upon hole and electron doping [7,37] it would be premature to suggests a shift in the case of GRA or GO.[33,35,36] We will address this while discussing the electrical measurement more clearly. Notably, the spectral location of G^{GRA}_{Atm}, G^{GO}_{Atm}, D^{GRA}_{Atm} and D^{GO}_{Atm} cases represent a combined effect from the electron donating or withdrawing gaseous molecules in the atmosphere while δ_G or δ_D is an ensemble effect from a laser spot of ~300 nm diameter.

As outlined in the introduction two charge transfer mechanisms are feasible, however the dangling orbitals are more prone for hybridization which is dependent of course on the extent of orbital overlap.[5] Furthermore, the difference in the electronegativity of the atoms in the proximity of the surface govern the polarity and the magnitude of the bond dipole in the background of inductive effect from neighboring groups. The interacting orbitals of GRA are chemically different from that of GO due to its oxygen containing functional groups.[25] Note that unoxidized portions of GRA still exists in GO. Hence in GO case surface adsorption of guest molecules would be position dependent where the functional groups and their intrinsic nature play a major role.[3,14]

In an earlier study [11] the sensor is treated with test liquids directly, while here we have exposed it to the test vapors. In the former case the molecules are physically existing on the surface in contrast the test molecules are in equilibrium state and electronically interacting. The *IV*-spectra from GRA and GO devices under three different environments are shown in Figure 4 on semilog scale and in Figure S4 of ESI on linear scale. The results of linear fit close to zero bias are tabulated in Figure S5 of ESI. From Figure 4, for similar bias condition the current carried by GRA is nearly three orders higher than its oxide counterpart for similar device dimensions. The reason for increased resistance is nothing but oxidation, where it disrupts the sp^2 conjugation and the conduction takes place via isolated sp^2 clusters. If we keep aside the quantitative differences, it is also inferred that under exposure to EtOH or IPA vapors the resistance of the GRA-device increases in contrast to that of GO-device which has shown decreased resistance. The quantitative response (ΔR^{Host}_{Guest}) from each device and the band diagram are shown in Figure 5a and b, respectively. The increase in the resistance is denoted by $^{+}$sign while decrease is denoted by $^{-}$ve sign. The phenomenon that takes place causing contrasting behavior of GRA and GO is rather complex and discussed in the following although Raman spectra indicates a transfer of charge among *guest* and *host.* Furthermore, in contrast to Ref [11], GRA and GO-devices have shown nonlinear response (Figure S4 of ESI) for higher bias conditions which suggests the variation in the conduction mechanism and warrants further investigation. On the other hand, the surface adsorption of the *guest* molecules might not be uniform throughout the surface of GO due to the band bending and associated charge accumulation, see Figure 5b.

In plane and out of plane conductivities are cumulatively reflected in GRA-device [38] where there exists a π-π interaction (*d* = ~3.368 Å) between the sheets (Figure 5c). This is in contrast to GO-device, where the charge carrier delocalization is limited to the surface via sp^2 domains, however, may be not across the

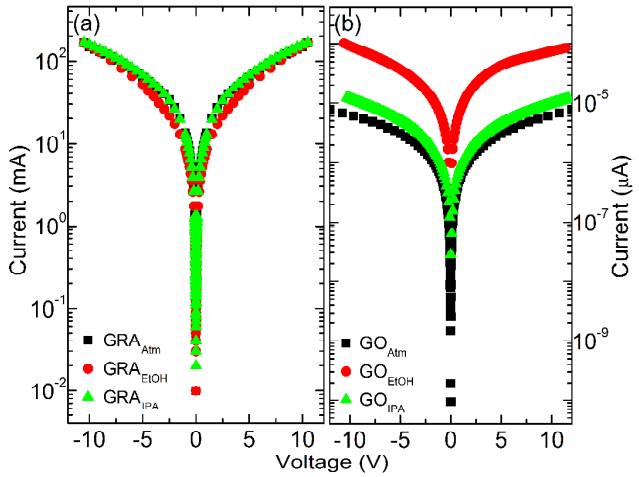

Fig. 4 (Color online) IV-characteristics of the devices in three different environments for (a) GRA and (b) GO on semilog plot.

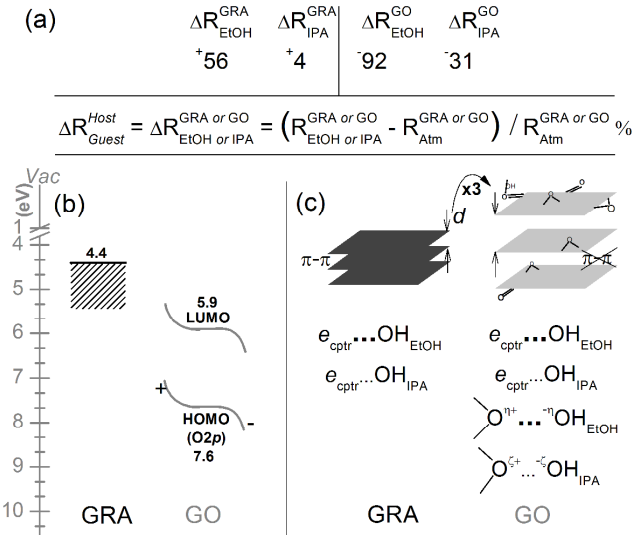

Fig. 5 (a) Quantitative response (ΔR_{Guest}^{Host}) from GRA and GO-devices, schematic of (b) energetic locations taken from literature [32,33,36,39,40] and (c) mechanism of *host-guest* interactions where e^-_{cptr}-electron capture, OH_{EtOH} and OH_{IPA} are -OH functional groups in EtOH and IPA respectively. Linear fit on the *IV*-characteristics are performed close to the zero bias and the resistance is employed in the above relation.

sheets (d = ~9.135 Å) as prominent as in the case of GRA. Under exposure to *guest* molecules, ΔR_{Guest}^{Host} from these devices is mutually contrasting, *viz* +ve and –ve ΔR for GRA and GO cases, respectively. The +ve ΔR_{Guest}^{GRA} is because of decreased carrier-carrier scattering when some of the electrons are captured (e^-_{cptr}) by *guest* molecules (Figure 5c). If e^-_{cptr} takes place via relatively stronger bond then as expected $\Delta R_{EtOH}^{GRA} > \Delta R_{IPA}^{GRA}$ in the light of differences in the acidic nature of *guest* molecules, *c.f.* $|\eta| > |\zeta|$. e^-_{cptr} takes place in the case of GO also, however, additionally *guest* molecules can form a dipole-type bond with epoxy groups (Figure 5c). However, geometric orientation and kinetics therein play a major role in the e^-_{cptr} and interaction with functional groups.[3,5,14] Furthermore $\Delta R_{EtOH}^{GRA} < \Delta R_{EtOH}^{GO}$ is because of the intrinsic nature of the *host* materials and elaborated in the following. To transform electron rich material into a *p*-type material, in principle the free *electrons* should be withdrawn in addition to those paired with *holes*. For GO-device the level of oxidation determines the nature of conduction.[33] If all of the *electrons* are not withdrawn by the functional groups then the majority carriers are still *electrons* although not as dense as parent GRA. Such low density of electrons when subjected to e^-_{cptr} process results in a significant conductance changes. Note the other possibility of transfer of *electrons* from *guest* to the relatively more acidic functional groups (other than epoxy) lead to an increase in the density of electrons in GO thereby increase in the conductance (i.e. +ve ΔR_{Guest}^{GrO}). Since ΔR_{Guest}^{GO} is not +ve the only possibility is e^-_{cptr} by *guest* molecules and hence the observation of $\Delta R_{EtOH}^{GRA} < \Delta R_{EtOH}^{GO}$ is satisfied. On the other hand if the GO is a complete *p*-type material, then the majority carriers are *holes* in which case the interaction of *guest* with epoxy functional groups is predominant. This interaction causes a shift of charge from GO to *guests* increasing the conductance. Moreover, other functional groups which are more acidic than EtOH can withdraw electrons from *guests* there by partially neutralizing or at least trapping the *holes* which decreases the conductance (-ve ΔR_{Guest}^{GO}). Having said that it may not be possible to rule out any of the above interactions between functional groups and *guest* molecules, where an integral effect is reflected in the *IV*-spectra.

Raman spectra at selected bias conditions are shown in Figure S6 of ESI for GRA and GO cases under three different environments. As mentioned earlier, Basko suggested that A(2D)/A(G) is almost invariant for GRA in field effect configuration.[41] In this direction, we have performed similar analysis and the results are shown in Figure S7 of ESI. It would be appropriate to discuss the reasons for the variation and changes in the trends for three cases as it requires foreknowledge of behavior of G and D bands in the presence of test vapors. Moving to the main motto of this report, we believe that it would be rather useful to consider the defect scattering in GRA and GO especially in the context of molecular charge transfer in a simple resistive type sensor. The results of *host-guest* chemistry on $A(G_{Guest}^{Host})$ and $A(D_{Guest}^{Host})$ are shown in Figure S8 of ESI for both bias conditions. The symmetric response is expected as the device has symmetric structure (Figure S1 of ESI)..For better representation only one polarity is shown in Figure 6. Crudely, at relatively higher bias condition (> 9 V) all cases have shown a kind of saturation towards low and high intensity for GRA and GO cases respectively, *c.f.* +ve ΔR_{Guest}^{GRA} and -ve ΔR_{Guest}^{GO}. However, the features appeared like a process with two transitions. $A(G_{Atm}^{GRA})$ is almost constant until ~0.01V and then fallen rapidly with increasing bias. After this sudden fall, $A(G_{Atm}^{GRA})$ and $A(G_{IPA}^{GRA})$ have retraced each other and appeared like they are saturating (Figure 6a) at relatively higher bias. Notably $A(G_{EtOH}^{GRA})$ stayed within 0.6 to 1 on the normalized scale for all bias conditions, while the transition has taken place slightly < 0.1V after which it has decreased. Quite distinctively, two transitions can be seen for $A(G_{Guest}^{GO})$ yielding intensity levels which are initially constant, sudden rise and almost constant, in the said sequence (Figure 6b). Moving onto the defect activated D band, $A(D_{Atm}^{GRA})$ has shown two clear transitions and however not retracing the $A(D_{IPA}^{GRA})$ as its G counterpart did. On the other hand $A(D_{EtOH}^{GRA})$ case is similar to its G band counterpart. The

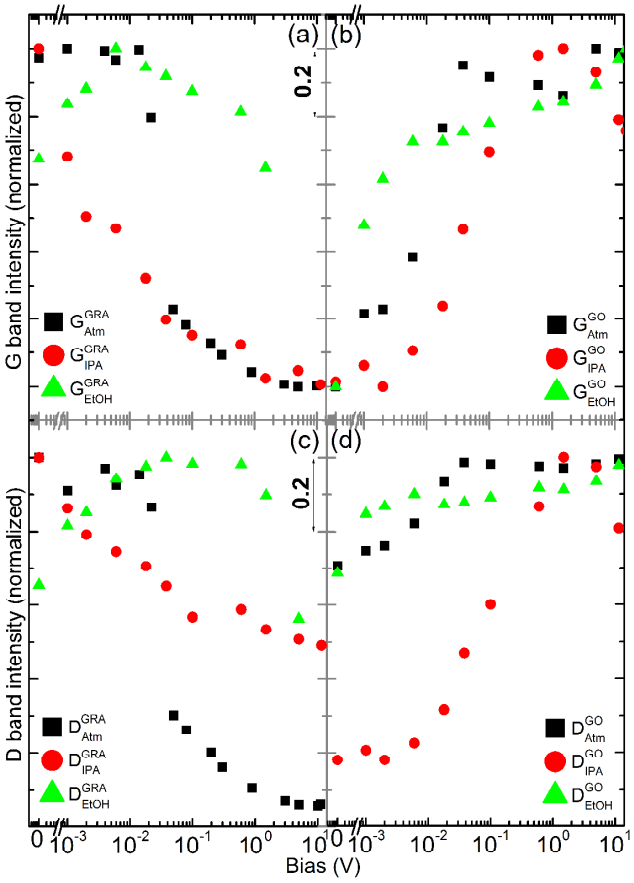

Fig. 6 (Color online) Raman intensities for three environments. G band from (a) GRA, (b) GO; D band from (c) GRA and (d) GO. The spectra are normalized against the intensity at zero bias. 0V is manually assigned on the log scale.

behavior from $A(D^{GO}_{Atm})$ and $A(D^{GO}_{EtOH})$ is comparable with an exception of the transition, where they appear to saturate from ~ 0.006 V and ~0.04 V respectively. $A(D^{GO}_{IPA})$ has almost shown two transitions similar to $A(G^{GRA}_{Atm})$ and $A(G^{GO}_{IPA})$. The reasons for this peculiar though interesting behavior is explained in the following.

In a broader context, the changes in carrier concentration and mobility alters the phonon dispersions and its intensity.[6-8] Largely similar behavior of $A(G^{GRA}_{Atm})$ and $A(G^{GRA}_{IPA})$ can be due to the weak interaction between *host* and *guest* similar to the gases in the atmosphere. While, the behavioral difference between $A(G^{GRA}_{IPA})$ and $A(G^{GRA}_{EtOH})$ can be due to the variance in e^-_{cptr} efficiency. These are notably, related to geometry of the molecule and the location on the surface.[3,5,14] The overall trend of intensity changes with increasing bias can be understood in conjunction with the *host-guest* interactions and nonlinear *IV*-response. The nonlinear *IV* suggests the varying resistance of the device with voltage. As the voltage increases the higher electric field perhaps pull the electrons back into the system. This is applicable to both GRA and GO devices. In the case of GRA, increase of charge carrier density increases the scattering and decreases the intensity of G or D bands. For GO case, since the electron density in GO is quite low, relatively higher bias conditions increases the electron density and hence the intensity of G or D band.

The multistep process can be because of the differences in the binding of energy of captured electron which were released back into the system at different bias conditions. In connection to the interaction with functional groups (GO case) it would be rather difficult to unambiguously determine the breakage of these interacting bonds. Earlier we have discussed that EtOH can strongly bind to the surface in e^-_{cptr} process ($|\eta| > |\zeta|$). Stronger binding may not necessarily reflect a complete transfer of electrons. The case with EtOH is quite interesting in both GRA and GO cases as it has shown one transition for all four contexts. This suggests that the EtOH molecules form two types of bonds with the surface. If we see the results from GO it appears to be the case that Atm and EtOH are similarly working in clear contrast to IPA case, where the second transition for $A(G^{GO}_{IPA})$ is at ~1V. Hence IPA perhaps binds to the surface by e^-_{cptr} with two binding energies. As mentioned earlier, in the following we discuss the reasons for the variation in the trends of A(2D)/A(G).

In field-effect-configuration, the E_F is manipulated via changing the gate voltage, which can be controlled externally. By given the present device structure is similar to top gate configuration the gate voltage is analogous to the transfer of charge by the *guest* molecules. Interestingly, A(2D)/A(G) is not constant either for GRA or GO cases. This suggests that the gate voltage applied by the molecular charge transfer may not be constant for all bias conditions. When the *guest* molecules are interacting with the defects the intensity changes in 2D band are expected. Hence the different trends in the A(2D)/A(G) for three cases is because of the variations within the molecules and the way they interact with the surface. As explained earlier, when it comes to equilibrium molecular doping, as in the present case, the molecules are bound to the surface within the lines of thermodynamic equilibrium, where their binding energy against applied bias needs to be taken into consideration. This is the core of various reasons for different trends seen in Fig. S7 of ESI. To emphasize, the surface binding depends on the 'molecule' its orientation and physical location (in case if it prefers a 'defect'). Earlier discussed points such as $|\eta| > |\zeta|$ and voltage dependent molecular desorption etc should also be taken into account. By given the above complexity the variations those were observed from Figure S7 of ESI demands further investigation.

Conclusions

In this report, we have studied electron phonon interactions from GRA and GO in a simple resistive type sensor. These sensors were exposed to saturated EtOH or IPA vapors under biased condition. We have focused on the change of the Raman intensity of the G and D bands as a function of the bias across the device in the presence of test vapors. Upon exposure to either EtOH or IPA softening of phonons is observed, where the *guest* molecules withdrawn electrons from both devices. Despite, we have noticed mutually contrasting changes in resistance for GRA and GO devices. These devices have shown nonlinear *IV*-response in contrast to the existing literature. For the case of GRA-device the resistance is decreased due to a decline in the carrier-carrier scattering, with the effect of the *guest* molecules capturing free electrons. The situation is completely different for GO device, where the resistance of the device is increased because of complex interactions such as dipole-type bonds apart from e^-_{cptr} process similar to GRA. The consequence of these interactions and possibility of involvement of other functional groups are addressed. Furthermore the quantitative response from

GRA is lower than GO, where the intrinsic nature of the *host* materials play a crucial role. The intensity changes of D and G bands, we believe to be rather crucial to be investigated and we note that A(2D)/A(G) is not invariant for GRA in the present equilibrium top gate-like configuration. Broadly, the intensities behaved contrasting to each other which can be treated similar to the change in the resistance under exposure to *guest* molecules. We note that this intensity changes are not because of the solvent intercalation. $A(G^{GRA}_{Guest})$ and $A(D^{GRA}_{Guest})$ were initially constant with bias and then fallen rapidly at higher bias condition and depicted a kind of saturation. Note that EtOH and IPA were exceptions in this context, which have shown one transition, i.e. only two features. $A(G^{GO}_{Guest})$ and $A(D^{GO}_{Guest})$ were increased with increasing bias and shown a saturation at relatively higher bias. $A(D^{GO}_{IPA})$ has shown clear features of two transitions, i.e. initially constant then rapid increase to saturate finally. This is not seen for either EtOH or Atm cases explicitly. The results suggests that the onset of each step depends on the *guest* species and their nature of bonding on the surface. Essentially the binding energy against applied bias is crucial which determines the transition.

In the case of GO the surface adsorption of the *guest* molecules needs to be considered carefully, as they might not adsorb uniformly due to the band bending (under bias) and associated charge accumulation. Furthermore, the interaction of *guest* molecules with functional groups other than 'epoxy' is another factor that requires reasonable attention. This needs to be juxtaposed with the geometric orientation of the *guest* molecules. Due to the interaction of epoxy and *guest* molecules the HOMO level may face a shift due to the modified electron occupancy, however, it can be inferred from sophisticated simulation studies. See for example, H_2O, NH_3, CO, NO and NO_2 on graphene are studied for their absorption energies against adsorption position and orientation.[5]

Acknowledgements

S.V. thanks The Scientific & Technological Research Council of Turkey (TUBITAK) (TUBITAK-BIDEB 2221-Fellowships for Visiting Scientists and Scientists on Sabbatical) for postdoctoral fellowship. A.C. thanks TUBITAK-BIDEB for national PhD scholarship. TU acknowledges partial funding from EU FP7-Marie Curie-IRG NANOWEB (PIRG06-GA-2009-256428) and The Turkish Academy of Sciences–Outstanding Young Scientists Award Program (TUBA-GEBIP).

Notes and references

[a] *UNAM-National Nanotechnology Research Center, Bilkent University, Bilkent, Ankara, 06800 Turkey. Fax: +90 (312) 266 4365; Tel: +90 (312) 290 3584; E-mail: svempati01@qub.ac.uk*

[b] *Institute of Materials Science & Nanotechnology, Bilkent University, Bilkent, Ankara, 06800 Turkey Fax: +90 (312) 266 4365; Tel: +90 (312) 290 3571; E-mail: uyar@unam.bilkent.edu.tr*

† Electronic Supplementary Information (ESI) available: For GRA and GO cases: Device schematic, SEM images, XRD in the presence of EtOH vapor, *IV*-spectra and results of its linear fit, Raman spectra at selected bias conditions. Intensity ratios of 2D and G bands. G and D band intensity variations for either side of teh biases for all three cases. See DOI: 10.1039/b000000x/

1 F. Yavari and N. Koratkar, *J. Phys. Chem. Lett.*, 2012, **3**, 1746-1753.
2 F. Yavari, Z. Chen, A. V. Thomas, W. Ren, H.-M. Cheng and N. Koratkar, *Sci. Rep.*, 2011, **1**, 1-5.
3 F. Schedin, A. K. Geim, S. V. Morozov, E. W. Hill, P. Blake, M. I. Katsnelson and K. S. Novoselov, *Nat. Mater.*, 2007, **6**, 652-655.
4 H. J. Yoon, D. H. Jun, J. H. Yang, Z. Zhou, S. S. Yang and M. M.-C. Cheng, *Sens. Actu. B*, 2011, **157**, 310-313.
5 O. Leenaerts, B. Partoens and F. M. Peeters, *Phys. Rev. B.*, 2008, **77**, 125416(125411)-125416(125416).
6 M. Lazzeri and F. Mauri, *Phys. Rev. Lett.*, 2006, **97**, 266407(266401)-266407(266404).
7 S. Pisana, M. Lazzeri, C. Casiraghi, K. S. Novoselov, A. K. Geim, A. C. Ferrari and F. Mauri, *Nat. Mater.*, 2007, **6**, 198-201.
8 A. Das, S. Pisana, B. Chakraborty, S. Piscanec, S. K. Saha, U. V. Waghmare, K. S. Novoselov, H. R. Krishnamurthy, A. K. Geim, A. C. Ferrari and A. K. Sood, *Nat. Nanotech.*, 2008, **3**, 210-215.
9 D. M. Basko, S. Piscanec and A. C. Ferrari, *Phys. Rev. B*, 2009, **80**, 165413.
10 W. Chen, S. Chen, D. C. Qi, X. Y. Gao and A. T. S. Wee, *J. Am. Chem. Soc.*, 2007, **129**, 10418-10422.
11 B. Das, R. Voggu, C. S. Rout and C. N. R. Rao, *Chem. Commun.*, 2008, 5155–5157.
12 A. C. Ferrari and J. Robertson, *Phys. Rev. B*, 2000, **61**, 14095.
13 F. Tuinstra and J. L. Koenig, *J. Chem. Phys.*, 1970, **53**, 1126.
14 B. S. Gonzalez, J.H.-Rojas, J. Breton and J. M. G. Llorente, *J. Phys. Chem. C.*, 2007, **111**, 14862-14869.
15 K. Kahn and T. C. Bruice, *Chem. Phys. Chem.*, 2005, **6**, 487– 495.
16 S. You, S. Luzan, J. Yu, B. Sundqvist and A. V. Talyzin, *J. Phys. Chem. Lett.*, 2012, **3**, 812-817.
17 S. You, J. Yu, B. Sundqvist, L. A. Belyaeva, N. V. Avramenko, M. V. Korobov and A. V. Talyzin, *J. Phys. Chem. C.*, 2012, **117**, 1963-1968.
18 D. C. Marcano, D. V. Kosynkin, J. M. Berlin, A. Sinitskii, Z. Sun, A. Slesarev, L. B. Alemany, W. Lu and J. M. Tour, *ACS Nano*, 2010, **4**, 4806-4814.
19 H. A. Becerril, J. Mao, Z. Liu, R. M. Stoltenberg, Z. Bao and Y. Chen, *ACS Nano*, 2008, **2**, 463-470.
20 K. P. Loh, Q. Bao, P. K. Ang and J. Yang, *J. Mater. Chem*, 2010, **20**, 2277-2289.
21 F. M. Wenzhong Bao, Zhen Chen, Hang Zhang, Wanyoung Jang, Chris Dames & Chun Ning Lau, *Nat. Nanotechnol.*, 2009, **4**, 562-566.
22 D. Lee, J. Seo, X. Zhu, J. Lee, H.-J. Shin, J. M. Cole, T. Shin, J. Lee, H. Lee and H. Su, *Sci. Rep.*, 2013, **3**, 2250.
23 H. Lipson and A. R. Stokes, *Proc. R. Soc. A*, 1942, **181**, 101-105.
24 J. S. Kukesh and L. Pauling, *Am. Mineral.*, 1950, **35**, 125.
25 P. Johari and V. B. Shenoy, *ACS Nano*, 2011, **5**, 7640-7647.
26 A. C. Ferrari and D. M. Basko, *Nat. Nanotech.*, 2013, **8**, 235-246.
27 C. Thomsen and S. Reich, *Phys. Rev. Lett.*, 2000, **85**, 5214.
28 A. C. Ferrari, *Solid State Commun.*, 2007, **143**, 47-57.
29 S. Piscanec, M. Lazzeri, F. Mauri, A. C. Ferrari and J. Robertson, *Phys. Rev. Lett.*, 2004, **93**, 185503.
30 I. Pocsik, M. Hundhausen, M. Koos and L. Ley, *J. Non-Cryst. Solids*, 1998, **227-230**, 1083-1086.
31 R. P. Vidano, Fishbach, D. B., Willis, L. J., Loehr, T. M., *Solid State Comm.*, 1981, **39**, 341-344.
32 H.-K. Jeong, Y. P. Lee, R. J. W. E. Lahaye, M.-H. Park, K. H. An, I. J. Kim, C.-W. Yang, C. Y. Park, R. S. Ruoff and Y. H. Lee, *J. Am. Chem. Soc.*, 2008, **130**, 1362-1366.
33 R. J. W. E. Lahaye, H. K. Jeong, C. Y. Park and Y. H. Lee, *Phys. Rev. B*, 2009, **79**, 125435.
34 T. B. Szabo, O.; Forgo, P.; Josepovits, K.; Sanakis, Y.; Petridis, D.; Dekany, I., *Chem. Mater.*, 2006, **18**, 2740–2749.
35 X. Dong, D. Fu, W. Fang, Y. Shi, P. Chen and L.-J. li, *Small*, 2009, **5**, 1422-1426.
36 M. Jin, H.-K. Jeong, W. J. Yu, D. J. Bae, B. R. Kang and Y. H. Lee, *J. Phys. D: Appl. Phys.*, 2009, **42**, 135109.
37 J. Yan, Y. Zhang, P. Kim and A. Pinczuk, *Cond.Mat./0612634*, 2006.
38 G. H. Kinchin, *Proc. R. Soc. Lond., A*, 1952, **217**, 9-26.
39 G. K. Wertheim, P. M. T. M. V. Attekum and S. Basu, *Solid State Commun.*, 1980, **33**, 1127-1130.

40 D. Marchand, C. Fretigny, M. Lagues, F. Batallan, C. Simon, I. Rosenman and R. Pinchaux, *Phys. Rev. B*, 1984, **30**, 4788.
41 D. M. Basko, *Phys. Rev. B*, 2008, **78**, 125418.

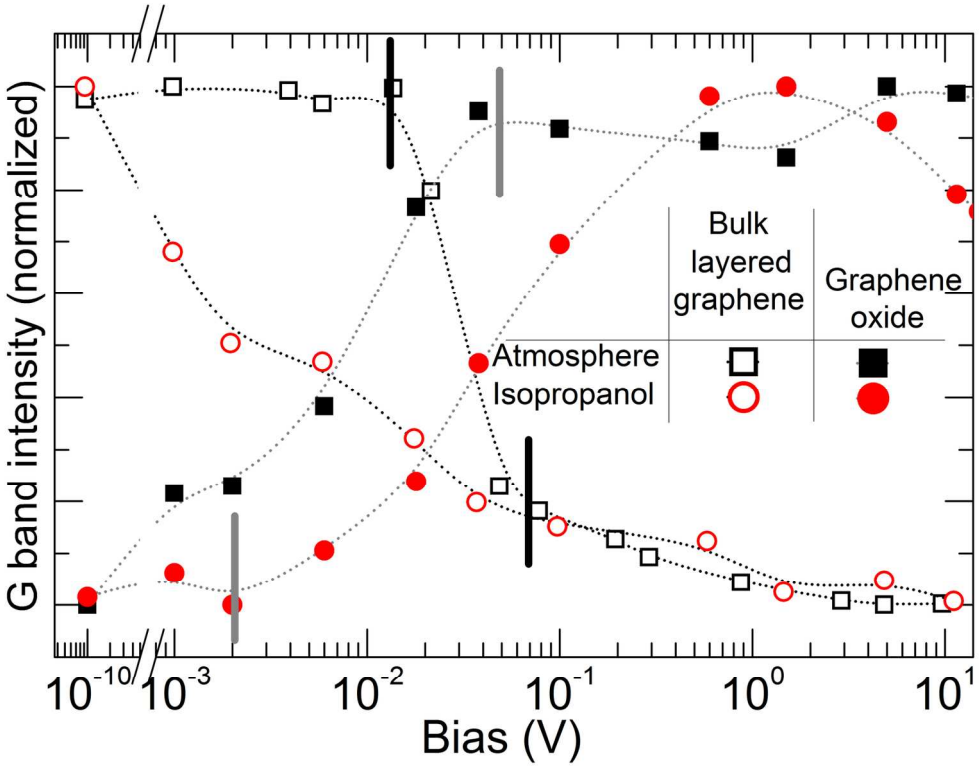

Intensity variation of G band from bulk layered graphene and its oxide in ambient or isopropanol vapor showing mutually contrasting behavior under bias.
152x117mm (300 x 300 DPI)